Appl Microbiol Biotechnol (2017) 101:817–829
DOI 10.1007/s00253-016-7914-9

ENVIRONMENTAL BIOTECHNOLOGY

16S rRNA gene-based characterization of bacteria potentially associated with phosphate and carbonate precipitation from a granular autotrophic nitrogen removal bioreactor

Alejandro Gonzalez-Martinez[1] · **Alejandro Rodriguez-Sanchez**[2] · **María Angustias Rivadeneyra**[3] · **Almudena Rivadeneyra**[4] · **Daniel Martin-Ramos**[5] · **Riku Vahala**[1] · **Jesús Gonzalez-Lopez**[2,6]

Received: 22 August 2016 / Accepted: 4 October 2016 / Published online: 3 November 2016

Abstract A bench-scale granular autotrophic nitrogen removal bioreactor (completely autotrophic nitrogen removal over nitrite (CANON) system) used for the treatment of synthetic wastewater was analyzed for the identification of microbiota with potential capacity for carbonate and phosphate biomineral formation. 16S ribosomal RNA (rRNA) gene-based studies revealed that different bacterial species found in the granular biomass could trigger the formation of phosphate and calcite minerals in the CANON bioreactor. iTag analysis of the microbial community in the granular biomass with potential ability to precipitate calcium carbonate and hydroxyapatite constituted around 0.79–1.32 % of total bacteria. Specifically, the possible hydroxyapatite-producing *Candidatus Accumulibacter* had a relative abundance of 0.36–0.38 % and was the highest phosphate-precipitating bacteria in the granular CANON system. With respect to calcite precipitation, the major potential producer was thought to be *Stenotrophomonas* with a 0.38–0.50 % relative abundance. In conclusion, our study showed evidences that the formation of hydroxyapatite and calcite crystals inside of the granular biomass of a CANON system for the treatment wastewater with high ammonium concentration was a biological process. Therefore, it could be suggested that microorganisms play an important role as a precipitation core and also modified the environment due to their metabolic activities.

Keywords Biomineralization · Calcite · CANON · Nitrogen · Phosphate · iTag

✉ Alejandro Gonzalez-Martinez
alejandro.gonzalezmartinez@aalto.fi

[1] Department of Civil and Environmental Engineering, Aalto University, P.O. Box 15200, Aalto, FI-00076 Espoo, Finland

[2] Department of Built Environment, Aalto University, Espoo, Finland

[3] Institute of Water Research, University of Granada, Granada, Spain

[4] Department of Microbiology, University of Granada, Granada, Spain

[5] Institute of Nanoelectronics, Technical University of Munich, Munich, Germany

[6] Department of Mineralogy and Petrology, University of Granada, Granada, Spain

Introduction

High levels of ammonium in domestic or industrial wastewater can cause eutrophication processes and oxygen depletion, as well as ecotoxicity over aquatic wildlife, and affect the suitability of discharged wastewater for reuse (Wang et al. 2010; Driscoll et al. 2012). Over the past few decades, ammonium has been eliminated from wastewater through conventional nitrification-denitrification technology, which oxidizes all ammonium to nitrate under autotrophic, aerobic conditions and then reduces nitrate to molecular nitrogen under heterotrophic, anaerobic conditions (Gonzalez-Martinez et al. 2011). Traditional nitrification-denitrification processes for nitrogen removal in wastewater treatment systems have to deal with high-energy requirements and the need of organic carbon source for nitrogen elimination; moreover, these technologies require a wide surface area for a proper setup; overcoming these disadvantages has been made possible by the development of anammox autotrophic nitrogen removal processes (Zhu et al. 2008; Ali and Okabe 2015; Xu et al. 2015; Xing et al. 2016).

The completely autotrophic nitrogen removal over nitrite (CANON) technology is one of the most novel, efficient, and promising wastewater treatment processes for the bioremediation of effluents with high ammonium concentration and low

organic carbon content. The development of granular biomass in these systems support the elimination nitrogen by ammonium oxidation to nitrite carried out by ammonium-oxidizing bacteria and subsequent anammox pathway which converts ammonium and nitrite into molecular nitrogen inside the same bioreactor (Zhang et al. 2013; Zhang et al. 2015).

The presence of mineral crystals in granular biomass, both from CANON systems and aerobic granular processes, has been previously reported (Mañas et al. 2012; Lin et al. 2013). In addition, positive correlations between granular biomass mechanical properties and formation of mineral crystals inside them have been proposed, mainly concerning enhanced physical strength of the granule against compression and density (Lin et al. 2013; Winkler et al. 2013). Therefore, the formation of mineral crystals in granular biomass processes, such as the CANON technology, has been considered as beneficial for the purpose of treatment, enhancing durability of granular biomass and its settling capacity. However, it is not known if the process of formation of these minerals is associated with the biological activity of the microbiota or simply is a process independent of it.

It has been suggested that bacteria play a significant role in the formation of a diversity of minerals in natural and engineered environments (Ehrlich and Newman 2009; Gonzalez-Martinez et al. 2015a). This biological process has been named biomineralization. Biomineralization is a biological process in which microorganisms play a role in the formation of minerals and changes different microenvironmental parameters such as pH and ion concentrations (Elrich and Newman 2009). In this sense, it has been proposed that there are species-specific associations with the minerals whose formation is mediated by microorganisms, i.e., formation of a given mineral would be mediated by a certain number of bacterial strains, although is also true that biomineralization processes may simply be associated with environmental changes caused by microbial activity without any species-specific association (Gonzalez-Martinez et al. 2015a). In this context, the presence of mineral crystals in the granular biomass could be explained by the activity of microorganisms.

The most frequent and important minerals produced by bacteria isolated from wastewater treatment plants are carbonates (particularly as calcite and vaterite) and phosphates (mainly as struvite). The precipitation of phosphates in wastewater treatment technologies is of great interest which gives additional values to wastewater treatment processes (Soares et al. 2014; Crutchik and Garrido 2016; Lu et al. 2016). Moreover, it has been reported as a pathway for phosphate elimination from wastewater (Crystale et al. 2016). The emission of CO_2 to the atmosphere has been identified as the most important cause of climate change and global warming between 1750 and 2005 (Luo and Wu 2015). In this sense, the carbonate precipitation in wastewater and the formation of carbonate biominerals could sequestrate in some part the CO_2 released to the atmosphere by human activities.

In this study, granules of a CANON bioreactor were analyzed for the presence of mineral crystals. As well, the bacterial community structure of this biomass has been analyzed by the means of iTag sequencing procedure to explore the diversity of bacteria that can trigger the formation of minerals found within it. The results show the composition of the crystals and that the relative abundance of potential crystal-precipitating bacteria, although low in comparison with the major players in nitrogen removal in the system, attained a high relevance within the bacterial community structure of the granule. However, an important objective of our study was to show if crystal formation was associated with the biological activity of the granular biomass. In this sense, experiences with an inoculated bioreactor, a bioreactor inoculated with autoclaved granular biomass, and a bioreactor inoculated with metabolically active granular biomass were performed.

Materials and methods

CANON bioreactor setup and operation

A bench-scale CANON bioreactor was set up and inoculated for the experiment (Fig. 1). The inoculum consisted on granular sludge from a lab-scale CANON bioreactor operating at 35 °C. The characteristics and operational conditions of the CANON bioreactor can be seen in Table 1. Oxygen was supplied as a continuous aeration, with dissolved oxygen concentration controlled at 1 mg O_2 L^{-1}, because this value has been reported as optimum for CANON bioreactor operation (Hao et al. 2002). Also, influent synthetic wastewater feeding the CANON bioreactor had the same composition used by Gonzalez-Martinez et al. (2016a), which is shown in Table 2. The experiment was started when the inoculated CANON operated under steady-state conditions during a month. Then, the CANON bioreactor was continuously fed with wastewater from day 1 to day 120. Furthermore, pH and temperature were measured in the influent and effluent using a multimeter.

Biological sample collection

Granular biomass samples of 100 mL were collected from the CANON bioreactor once a week during 2 weeks after a 120-day operation period. Five biomass samples from five evenly distributed points in the bioreactor's volume were taken, following previous methodology (Gonzalez-Martinez et al. 2016b). The biomass was then submerged into 0.9 % NaCl saline solution. Solid and liquid phases

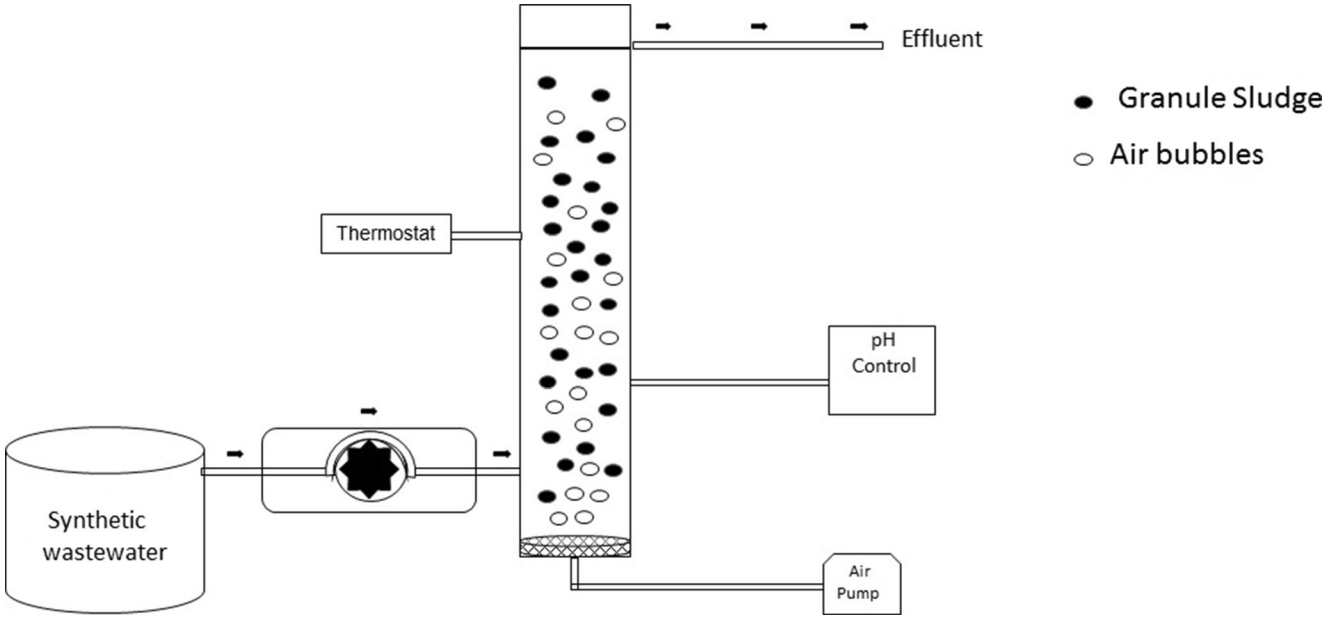

Fig. 1 Schematic representation of the CANON bioreactor

of the samples were separated by the means of centrifugation at 3500 rpm during 20 min at room temperature. The liquid supernatant was discarded, and pelleted biomass was then stored at −20 °C for further DNA extraction.

Study of mineral formation in the granular biomass

The granular biomass obtained from the CANON bioreactor samples was examined with an optical microscope for the presence of minerals up to 14 days after bioreactor inoculation. The experiments were carried out in triplicate and were repeated twice. A control consisting of uninoculated bioreactor and a bioreactor inoculated with autoclaved granular biomass were included in all the experiments.

Table 1 Design characteristics and operational conditions of the CANON bioreactor

Parameter	Amount	Units
Bioreactor volume	2	L
HRT	4	h
Dissolved oxygen (DO)	1	mg L^{-1}
pH	7.5	
Temperature	35 ± 1	°C
Total influent nitrogen	466 ± 12	mg N L^{-1}
Total effluent nitrogen	63 ± 24	mg N L^{-1}
Effluent NH_4^+-N L^{-1}	40 ± 13	mg N L^{-1}
Effluent NO_2^--N L^{-1}	3 ± 2	mg N L^{-1}
Effluent NO_3^--N L^{-1}	24 ± 6	mg N L^{-1}
Nitrogen removal	85 ± 2	%

Isolation and purification of the precipitates

For the mineralogical and morphological studies, precipitates formed in the CANON bioreactor were removed from the granular biomass by sonication in a bath sonicator (Ultrasonic batch, Selecta, Barcelona, Spain) at room temperature for 2 min at 40 kHz (0.05 W mL^{-1}). Mineral crystals were extracted by means of a small spatula and washed with distilled water to remove impurities and finally air-dried at 37 °C.

XRD studies

The minerals were analyzed by powder X-ray diffraction (PXRD) using a Philips PW 1710/00 diffractometer with a graphite monochromator automatic slit, CuKaα radiation, and an online connection with a microcomputer. Data were collected for a 0.4-s integration time in 0.02 °C 2θ interval between 3 and 80 °C. Data were processed using the XPPower program for a qualitative and quantitative determination of the mineral composition (Martin 2004). For quantitative analysis,

Table 2 Synthetic wastewater composition

Compounds	Amount (mg L^{-1})
$(NH_4)_2SO_4$	2350
$NaHCO_3$ (mg L^{-1})	3250
$CaCl_2$ (mg L^{-1})	300
KH_2PO_4 (mg L^{-1})	70
$MgSO_4$ (mg L^{-1})	20
$FeSO_4 \cdot 7H_2O$ (mg L^{-1})	9
H_2SO_4 (mg L^{-1})	5

full diffraction profiles of the experimental diffractograms were adjusted to weighted mixtures of the individual pattern phases. The crystalline mosaic size on hkl reciprocal vectors was obtained from full width at half the maximum (FWHM) intensity after instrumental broadening and Kα2 corrections.

SEM studies

Electron micrographs of the precipitates were made with carbon-coated samples using a high-resolution field emission scanning electron microscopy (FESEM) Carl Zeiss, Supra 40 V (Carl Zeiss, Oberlocken, Germany). Selected samples also coated with carbon were analyzed using energy-dispersive X-ray microanalysis (EDX, Aztec 350, Oxford Instruments, Abingdon, UK).

DNA extraction and iTag sequencing process

Then, ten subsamples, five for each sampling day (127 and 134 days of operation) of each bioreactor, were treated as independent samples for DNA extraction purposes. Five hundred milligrams of pelleted biomass of each sample was collected for DNA extraction using the FastDNA SPIN Kit for Soil (MP Biomedicals, Solon, OH). For each of the sampling dates, its five corresponding DNA extracts were merged into a DNA pool named CA (day 127) and CB (day 134) samples (Gonzalez-Martinez et al. 2016b). The pools of extracted DNA were then kept at −20 °C and sent to Research and Testing Laboratory (Lubbock, TX, USA) for further iTag sequencing process. This was done using the iTag apparatus and the Illumina reagent v3 kit. The primers 28F and 519R (5′-GAGTTTGATCNTGGCTCAG-3′ and 5′-GTNTTACNGCGGCKGCTG-3, respectively) (Gonzalez-Martinez et al. 2016a) were used to amplify the hypervariable regions V1–V3 of the 16S ribosomal RNA (rRNA) gene of *bacteria*. The iTag sequencing amplification followed the steps: 3 min at 94 °C; then 32 cycles of 30 s at 94 °C, 40 s at 60 °C, and 60 s at 72 °C; and final elongation step of 5 min at 72 °C.

iTag sequencing data pipeline and ecology analysis of biological samples

The raw sequences obtained through the iTag sequencing were processed using mothur v1.34.4 (Schloss et al. 2009). The following pipeline was done for CA and CB samples independently. Raw sequences were merged into contigs, and then, those were subjected to a screening in order to avoid sequences with more than zero ambiguous bases. Remaining sequences were then aligned against the SiLVA SEED v119 alignment. Aligned sequences were then screened in order to eliminate (i) sequences with more than eight homopolymers, (ii) sequences that failed to align at the position of forward primer, and (iii) sequences whose alignment ended further than the 95 % of total sequences. Remaining aligned sequences were then preclustered (Huse et al. 2010) and then checked for chimeras using UCHIME v4.1 (Edgar et al. 2011) implemented in mothur v1.34.4, which were then eliminated. The number of high-quality sequences remaining in CA and CB was 14,868 and 12,979, respectively. To conduct an ecological

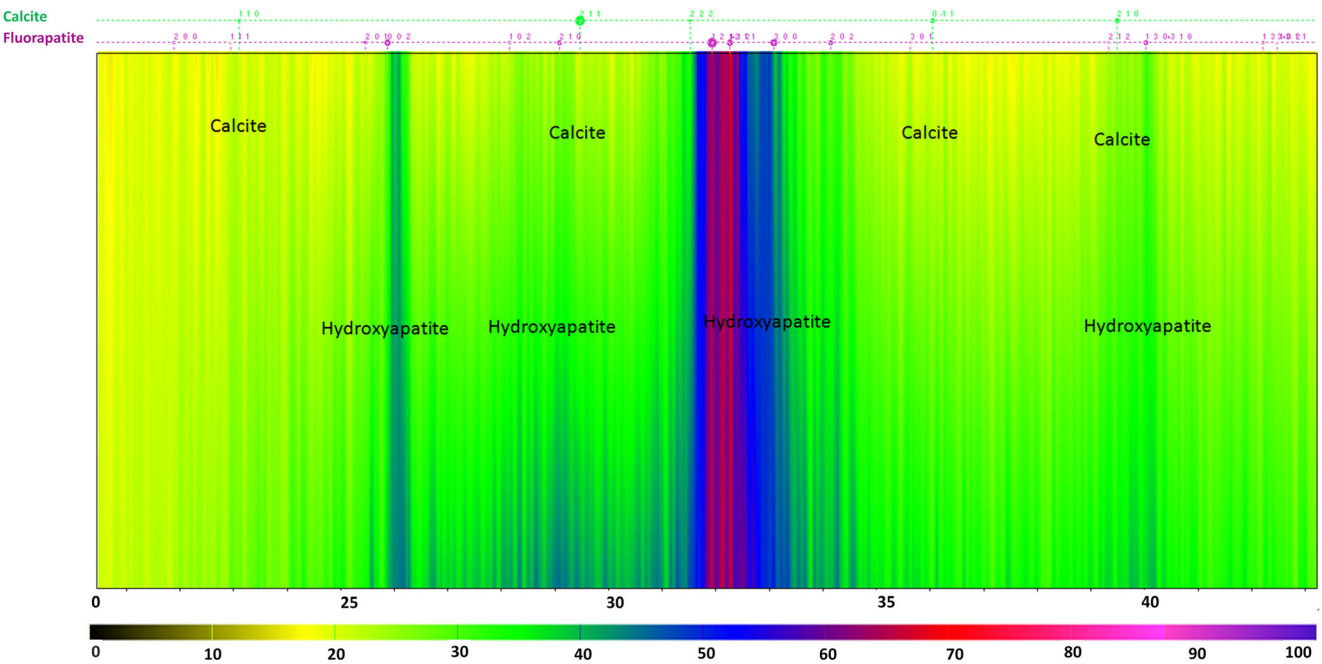

Fig. 2 Map drawn from XRD patterns. *Color* in the map indicates the changing intensity of the diffracted X-rays as a function of 2θ with warmer colors for progressively higher intensities. Characteristic bands of hydroxyapatite and calcite crystals are labeled in the graph

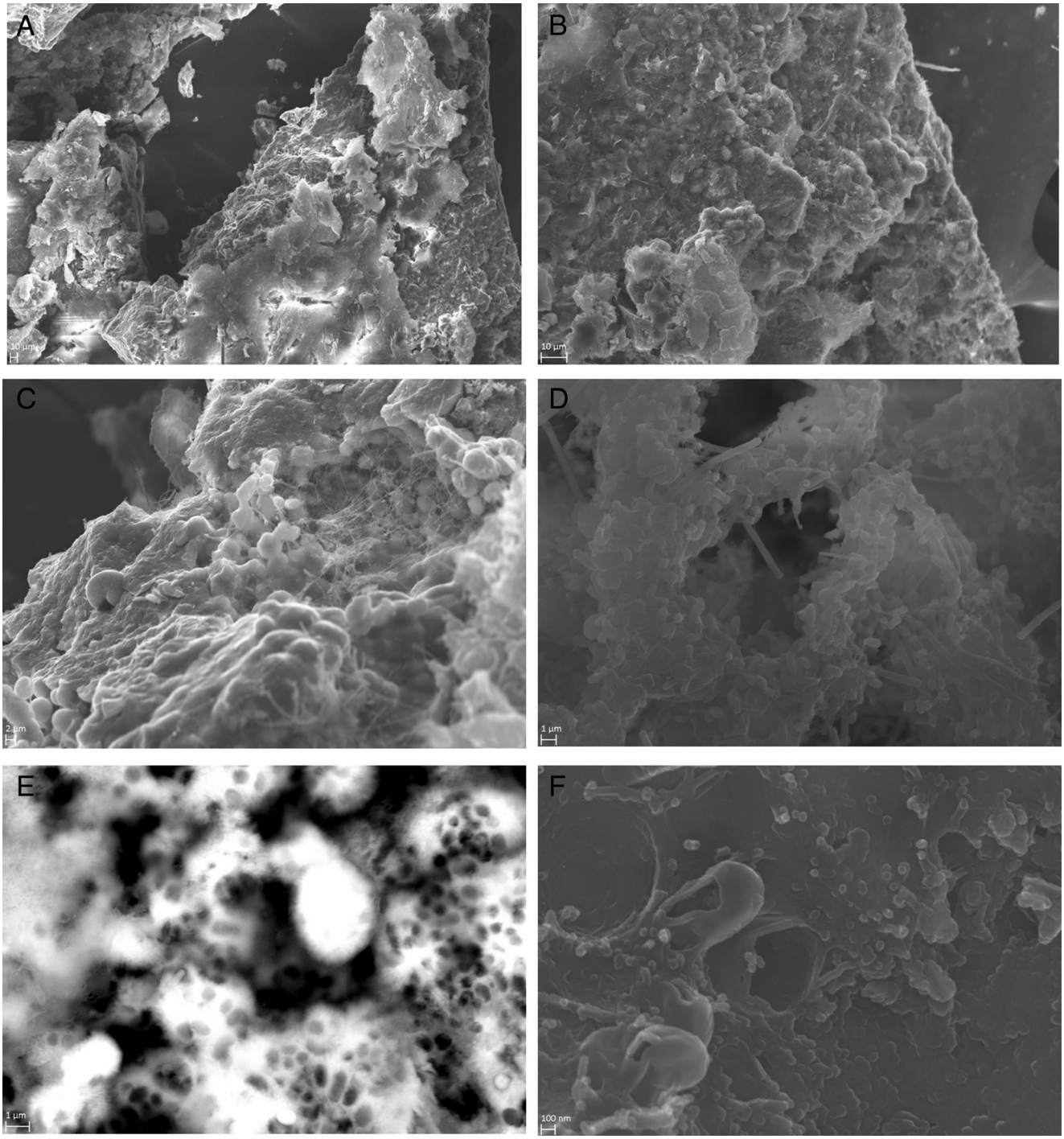

Fig. 3 FESEM images of mineralized granular biomass from the CANON bioreactor. **a**, **b** Mineralized granular biomass formed by calcified bacterial cells covered by a mucosal layer. **c**, **d** Close-up of **b**; note the abundance of mineralized bacterial cell covered by mucosed layer. **e** Detailed image of the calcified biomass showing many holes with bacteria-like size and shape. **f** Close-up of **d**; note the abundance of mineralized cells and nanoparticles delimiting the bacterial cells and mucosal layers

analysis, both samples were rarefied and cut to 12,979 sequences. After cut, both subsamples were subjected to a taxonomic affiliation following the operational taxonomic unit (OTU) approach separately. The sequences in each subsamples were used to generate a Phylip distance matrix, which was then taken for the OTU clustering of sequences in a 97 % similarity threshold. All OTUs were analyzed to determine the representative OTUs within each subsample. Representative OTUs were then taxonomically classified against the NCBI database. After taxonomic classification of OTUs, these were merged into consensus OTU taxonomy with an 80 % consensus confidence threshold.

Determination of coverage of iTag sequencing samples: complexity curves and redundancy abundance-weighted coverage analysis

The determination of the coverage of biological subsamples by iTag sequencing procedure and pipeline process was evaluated by the means of complexity curves and redundancy abundance-weighted coverage analysis. The complexity curves for each subsample were calculated by aRarefactWin software and took into account the counts of each of the consensus taxonomy OTU. The redundancy abundance-weighted coverage analysis was done by NonPareil software (Rodriguez-R and Konstantinidis 2014a). The data used was that of all sequences in the subsamples. The analysis was done by setting a 50 % sequence overlap, a 95 % sequence similarity, and query set size of 1000 sequences, as they are given as default parameters by the software.

α and β diversity analyses of iTag sequencing samples

Analyses of α and β diversity were done to check the similarity of samples in terms of bacterial diversity, evenness, and main species composition. Bacterial diversity and evenness were determined by the Hill diversity indices of order 1 (Shannon-Wiener index) and of order 2 (Simpson index), as they have been defended as the most robust diversity indices for the study of microbial communities (Haegeman et al. 2013). These were calculated using the counts of each of the consensus taxonomy OTU and through the vegan 2.0 package implemented in R-Project software. The similarity in major species composition was determined by the Morisita-Horn index (Barwell et al. 2015), which was calculated by the packages vegan 2.0 and vegetarian, both implemented in R-Project, and using the relative abundance data of each of the consensus taxonomy OTU.

Phylogenetic representation of most represented OTUs

A phylogenetic tree was developed to represent the taxonomic affiliation of representative OTUs with ≥0.50 % relative abundance in each of the subsamples. The sequences were aligned using the CLUSTALW algorithm, and the tree was calculated by 1000 bootstrap replications as test of phylogeny under the Jukes-Cantor substitution model in the neighbor-joining statistical method. All this was done using the MEGA6 software

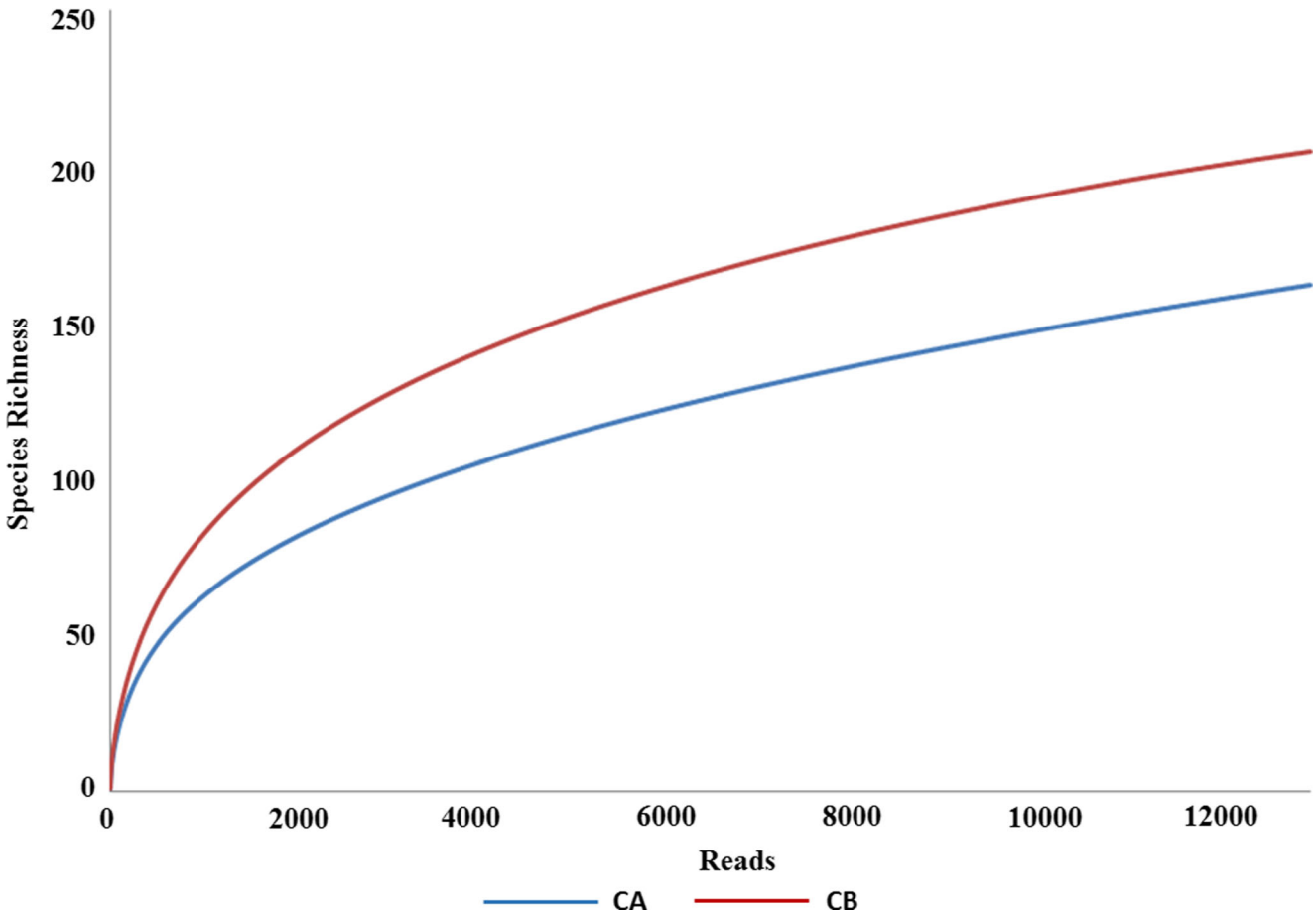

Fig. 4 Complexity curves of the CA and CB iTag sequencing subsamples

Table 3 Results of the redundancy abundance-weighted coverage analysis

Sample	Coverage (%)	Actual effort (Mbp)	Required effort (Kbp)
CA	96.91	12.19	907.3
CB	96.48	12.18	1060.0

(Tamura et al. 2013). The sequences represented in the phylogenetic tree were uploaded to the NCBI database under the accession numbers KX458069–KX458099.

Results

Performance of the CANON bioreactor through experimentation time

During the 120 days of operation under the same influent wastewater composition and in the temperature range of 35 ± 1 °C, the system achieved around 85 % nitrogen removal efficiency. NH_4^+, NO_2^-, and NO_3^- concentrations in the effluent were in the range of 40 ± 13 mg NH_4^+-N L^{-1}, 3 ± 2 mg NO_2^--N L^{-1}, and 24 ± 6 mg NO_3^--N L^{-1}, respectively (Table 1). This performance had constant values over time thanks to the constant operational conditions.

Mineral formation in the CANON system

The formation of mineral crystals in all the granular biomass took place rapidly, beginning 7 days after inoculation. After 14 days, the crystals significantly increased in quantity and were of a large size (more than 50 nm). However, no formation was observed in uninoculated control bioreactor or in the bioreactor inoculated with autoclaved granular biomass. These results show that the formation of mineral crystals occurs only in CANON bioreactor containing metabolically active granules.

The results of the mineralogical analysis with XRD (Fig. 2) showed that, in the granular biomass, hydroxyapatite was the main crystal precipitated (59.95 ± 2.00 %) although lower amounts of calcium carbonate as calcite were also produced (8.20 ± 5.20 %). It was also observed the formation of an important percentage of amorphous minerals (31.85 ± 3.5 %).

The morphology of the granular biomass observed by FESEM showed both mineralized components and non-mineralized components (Fig. 3). In this sense, when the mineralized components in the granular biomass were examined in detail, mineralized cells were observed frequently covered by mineralized exopolymeric substances.

Coverage analysis and diversity analysis of the iTag sequencing subsamples from the CANON bioreactor

The coverage analysis of the iTag sequencing subsamples was done by calculation of the complexity curve and redundancy abundance-weighted coverage values of each of them. The use of two different measures of coverage was done following the advice of previous literature (Rodriguez-R and Konstantinidis 2014b). The complexity curves of both subsamples reached saturation for the maximum number of reads, tending to a plateau (Fig. 4). Also, the values calculated for the redundancy abundance-weighted coverage analysis showed more than 96 % coverage for both subsamples (Table 3). In this sense, the iTag sequencing procedure was able to capture successfully the bacterial diversity of the bioreactor sampled.

The values of the Hill diversity index of order 1 were 2.868525 and 2.991492 for subsamples CA and CB; the Hill diversity index of order 2 had values of 0.8843279 and 0.8958097 for CA and CB, respectively. These were higher for the CB subsample (Table 4), which matches with the higher species richness observed for the CB subsamples in the complexity curve (Fig. 4) compared to the CA subsample. The similarity in the values of the α diversity indices showed that the iTag sequencing process yielded similar results in terms of bacterial community diversity for both subsamples. On the other hand, the values of the Morisita-Horn and symmetric indices were 0.9138233 and 0.2469136 (Table 4).

Bacterial community structure of the iTag sequencing subsamples from the CANON bioreactor

The bacterial community structure of >0.50 % consensus taxonomy OTUs of the iTag sequencing subsamples is shown in Table 5. The dominant phylotypes were affiliated to *Nitrosomonas* genus, *Planctomycetes* members, *Marinoscillum*, *Flavisolibacter*, and *Arenimonas* genera. *Nitrosomonas* could carry out the ammonium oxidation in

Table 4 Results of the α and β diversity analyses

				Morisita-Horn		Symmetric	
Sample	Shannon-Wiener	Simpson	Samples	CA	CB	CA	CB
CA	2.868525	0.8843279	CA	1	0.9138233	1	0.2469136
CB	2.991492	0.8958097	CB	0.9138233	1	0.2469136	1

Table 5 Relative abundances of >0.50 % consensus taxonomy OTUs in the CA and CB iTag sequencing subsamples

							Relative abundance (%)		
Domain	Phylum	Class	Order	Family	Genus	Species	CA	CB	Mean
Bacteria	*Acidobacteria*	environmental_samples	Unclassified	Unclassified	Unclassified	Unclassified	0.52	0.37	0.45
	Actinobacteria	*Actinobacteria*	*Actinomycetales*	*Cellulomonadaceae*	*Actinotalea*	Unclassified	0.56	0.09	0.33
	Bacteroidetes	environmental_samples	Unclassified	Unclassified	Unclassified	Unclassified	0.15	0.76	0.45
		Sphingobacteria	*Sphingobacteriales*	*Chitinophagaceae*	*Flavisolibacter*	Unclassified	4.86	13.45	9.16
					Terrimonas	Unclassified	1.91	1.70	1.80
				Cyclobacteriaceae	*Aquiflexum*	Unclassified	0.86	0.77	0.82
				Flexibacteraceae	*Arcicella*	environmental_samples	0.60	0.79	0.70
					Marinoscillum	Unclassified	12.20	13.65	12.92
	candidate_division_*OP10*	environmental_samples	Unclassified	Unclassified	Unclassified	Unclassified	1.07	0.58	0.82
	Gemmatimonadetes	environmental_samples	Unclassified	Unclassified	Unclassified	Unclassified	1.00	0.59	0.80
		Gemmatimonadales	*Gemmatimonadaceae*	*Gemmatimonas*	Unclassified	Unclassified	3.76	2.07	2.92
	Planctomycetes	environmental_samples	Unclassified	Unclassified	Unclassified	Unclassified	11.40	7.59	9.49
		Planctomycetia	*Candidatus Brocadiales*	Unclassified	Unclassified	Unclassified	2.71	6.81	4.76
				Candidatus Brocadiaceae	*Candidatus Scalindua*	*Candidatus Scalindua brodae*	1.31	0.68	1.00
	Proteobacteria	*Betaproteobacteria*	*Burkholderiales*	*Burkholderiaceae*	*Pandoraea*	environmental_samples	0.65	0.46	0.55
				Comamonadaceae	*Comamonas*	Unclassified	0.60	2.74	1.67
					Schlegelella	Unclassified	0.52	0.27	0.39
					Xenophilus	Unclassified	0.18	1.27	0.73
			Nitrosomonadales	*Nitrosomonadaceae*	*Nitrosomonas*	environmental_samples	5.97	9.46	7.72
						Unclassified	34.61	15.66	25.14
			Rhodocyclales	*Rhodocyclaceae*	*Azoarcus*	environmental_samples	0.58	0.23	0.40
					Candidatus Accumulibacter	Unclassified	0.36	0.68	0.52
		Gammaproteobacteria	*Xanthomonadales*	*Xanthomonadaceae*	*Arenimonas*	Unclassified	4.80	4.73	4.77
					Aspromonas	Unclassified	0.55	1.87	1.21
					Dokdonella	Unclassified	0.76	0.65	0.70
					Stenotrophomonas	environmental_samples	0.38	0.50	0.44
					Thermomonas	Unclassified	0.80	1.05	0.92
	Others						0.06	0.11	0.08

the system (Gonzalez-Martinez et al. 2016b), while *Arenimonas*, *Flavisolibacter*, and *Marinoscillum* were the heterotrophs responsible for generation of extracellular polymeric substance (EPS) and degradation of EPS and cell material through *N*-acetyl-D-glucosamine utilization (Kwon et al. 2007; Yoon and Im 2007; Seo et al. 2009; Huy et al. 2013; Cha et al. 2016). The unclassified *Planctomycete* consensus taxonomy was formed by several OTUs. Among them, one OTU in each of the samples had an 88–89 % similarity in a 97 % query cover with KU217839 *Candidatus Scalindua brodae Y4_Winter_56*, accounting for the 2.71 and 6.81 % relative abundance in samples CA and CB, respectively. Also, one OTU of each of the samples had a 97–98 % similarity with a 97 % query cover with the same *Candidatus Scalindua* clone KU217839 at 1.31 and 0.68 % relative abundance in the samples CA and CB. In this sense, these OTUs would belong to the *Candidatus Brocadiales* order and therefore would be anammox bacteria. Therefore, these OTUs could develop the anaerobic ammonium oxidation metabolism that would remove nitrogen in the CANON system (Yamagishi et al. 2013).

A phylogenetic tree showing the taxonomic affiliation of the >0.50 % OTUs in the system plus a representative OTU affiliated with phosphate-precipitating and calcite-precipitating bacteria *Candidatus Accumulibacter phosphatis*, *Stenotrophomonas*, *Bacillus*, and *Clostridium* are shown in Fig. 5. The phyla that contained the >0.50 % OTUs in both subsamples were *Bacteroidetes*, *Firmicutes*, *Proteobacteria*, and *Planctomycetes*. It can be seen that several OTUs found in the systems were correlated with *Nitrosomonas* strains, the ammonium-oxidizing genus in the CANON bioreactor. As well, *Planctomycete* phylum was divided into three branches. One of them represented OTUs associated with *Planctomycetes* found in anammox bioreactors such as AB775688, other represented known non-anammox *Planctomycetes* such as the *Planctomycete clone 5GA PLA HPK 17* (Park et al. 2010; Gonzalez-Martinez et al. 2015b), and other represented OTUs belonging to *Candidatus Brocadiales* order.

Discussion

Mineral formation in the CANON system

The results pointed out that the precipitation of minerals by microorganisms is common in the CANON granular biomass. Therefore, it is proposed that the precipitation through bacterial activity can take place when the wastewater has a high ionic concentration, and obviously, some microenvironmental parameters such as pH are modified by bacterial metabolism.

Numerous studies have demonstrated the microbial precipitation of carbonates and phosphates in different natural environments (Rivadeneyra et al. 2010; Gonzalez-Martinez et al. 2015a). Nevertheless, few papers have reported the bioprecipitation of these minerals (Uad et al. 2014; Rivadeneyra et al. 2014) by microbial strains in wastewater treatment systems, and, more specifically, there are no published reports of research in CANON systems. Most of the precipitates detected in the granular biomass showed rough surfaces (Fig. 3a, b). Moreover, the presence of many aggregates with bacteria-like size and shape confirmed that calcium precipitates were formed by the accumulation of calcified cells which are part of the biofilms (Fig. 3c, d). Also, calcium precipitates always observed inside the granular biomass suggested that microorganisms induced the bioprecipitation of calcium carbonate and calcium phosphate and play an important role as a precipitation core (e.g., biominerals form around the cell wall of the microorganisms), although also modified the environment due to their metabolic activities (pH and ion concentrations, Uad et al. 2014), increased thereby facilitating the mineral formation. Similar results have been reported in previous studies by Dupraz et al. (2004) and Rivadeneyra et al. (2010). Thus, the biological activity inside the granular biomass was considered essential in the biomineralization process. The importance of the metabolic activity of the microbiota in the granular biomass was also supported by the fact that no precipitation was produced in the control bioreactor inoculated with autoclaved (dead) granular biomass.

According to these results, it was suggested that in our CANON granular biomass used for the treatment of synthetic wastewater, the presence of high concentrations of phosphate, NH_4^+, and Ca^{2+} ions results in mineral bioprecipitation of hydroxyapatite. On the other hand, it was also evident that the release of lower amounts of CO_2 by heterotrophic microorganisms present in the granular biomass in the presence of Ca^{2+} induces the calcite precipitation. In this sense, the bioprecipitation of this mineral requires certain amounts of carbon dioxide, calcium, and appropriate pH (Uad et al. 2014). More detailed images of the precipitate surfaces (Fig. 3e, f) showed that mineralized cells were covered with calcium carbonate or calcium phosphate. According to Aloisi et al. (2006), the formation of nanoglobules is the first step in microbial precipitation. Thus, the presence of nanoglobules (nanoparticles) in the external bacterial envelopes (Fig. 3f) suggests that the microorganisms accumulated and precipitated calcium carbonate or calcium phosphate on the cell surface during bacterial growth and on exopolymeric components of the biofilms.

Bacterial community structure of the iTag sequencing subsamples from the CANON bioreactor

Nitrosomonas and *Planctomycetes* bacteria have been commonly found in CANON bioreactors studied through 454 pyrosequencing and DGGE (Gonzalez-Martinez et al. 2016b). The differences of this CANON bioreactor with other CANON systems studied by next-generation sequencing

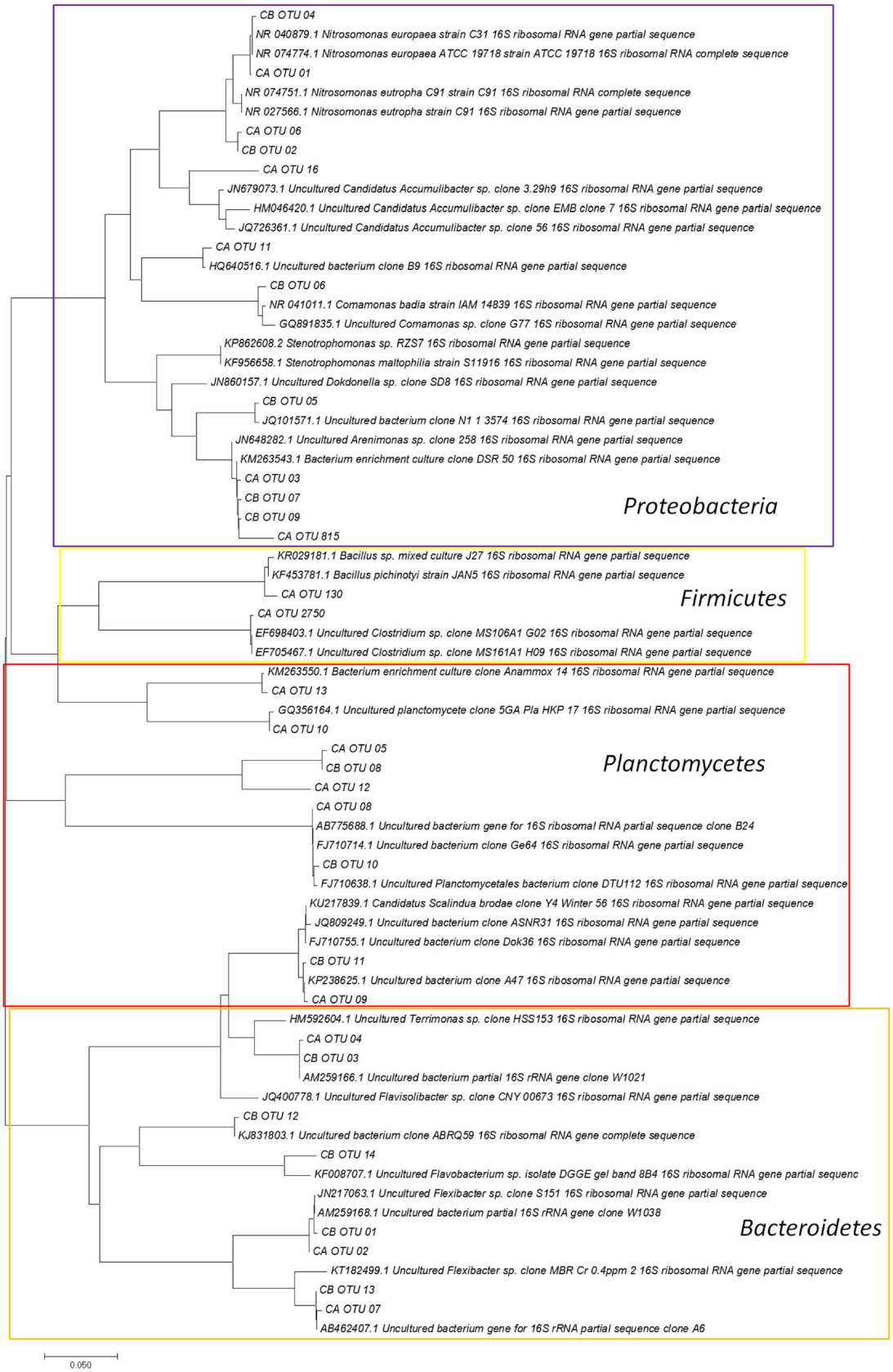

Fig. 5 Phylogenetic tree representing >0.50 % relative abundance OTUs in the CA and CB iTag sequencing subsamples and representative OTUs of the phosphate-precipitating and calcite-precipitating genera

reside in the diversity of satellite heterotrophs (Gonzalez-Martinez et al. 2016b). The adaptation of species of putative heterotrophs in both systems could be caused by differences in influent wastewater composition, aeration mechanisms (constant aeration versus intermittent aeration), operational temperature or pH, or differences in inoculum used for the start-up of the system, among others.

None of the genera found in the subsamples have been reported previously for mineral precipitation such as hydroxyapatite and calcite. Nevertheless, among all of the bacterial genera found, the best potential candidate for hydroxyapatite precipitation was *Accumulibacter*. *Candidatus Accumulibacter phosphatis* (CAP) is a bacterium frequently found in enhanced biological phosphorous removal (EBPR) systems. Currently, no cultured isolates of CAP exist, so the phylogeny of CAP strains is based purely of molecular biology techniques. This *Candidatus* species can store volatile fatty acids inside its cell membrane under anaerobic, rich carbon conditions, converting them to polyhydroxyalkanoates (PHAs) by the breakdown of previously stored polyphosphate (polyP); then, under aerobic, poor carbon conditions, the PHAs are degraded to provide carbon and energy for growth, as well as to replenish the utilized polyP (Oyserman et al. 2015). The capability of *Candidatus Accumulibacter* genus to store and degrade polyP could be related to hydroxyapatite nucleation. In this way, theories about biologically mediated hydroxyapatite formation state that initiation of hydroxyapatite crystals occurs when polyP is depolymerized in a Ca^{+2}-rich matrix (Omelon et al. 2013). The CANON bioreactor supports an environment in which Ca^{+2} and PO_4^- are present due to the composition of the influent synthetic wastewater. The accumulation of polyP inside the cell membrane of *Candidatus Accumulibacter* is possible due to the low organic carbon and microaerophilic conditions given in the inner parts of the granule. Again, due to the microaerophilic conditions in the granular biomass, the polyP could be degraded to store PHA. Thus, conditions in the CANON bioreactor could support both the growth of *Candidatus Accumulibacter* and the formation of hydroxyapatite crystals. This genus was found to be a 0.36 and 0.68 % in CA and CB subsamples, respectively.

Other bacterial species that have been reported for struvite precipitation, such as *Rhodobacter* and *Bacillus* (Gonzalez-Martinez et al. 2015a), were found in the CA and CB subsamples at low relative abundance—0.03 and 0.06 % for *Rhodobacter* in CA and CB subsamples and 0.09 and 0.02 % for *Bacillus* in CA and CB subsamples, respectively. These genera can trigger the formation of magnesium phosphate mineral struvite, so it is possible that they can also trigger the formation of calcium phosphate mineral apatite under the conditions given in the CANON bioreactor. Nevertheless, their relative abundances are low compared with that of *Candidatus Accumulibacter*, and therefore, the former seemed to be the major apatite precipitating bacteria found in the bioreactor.

The only major represented phylotype previously reported for calcite precipitation was *Stenotrophomonas* (Rusznyak et al. 2012; Park et al. 2013). Its relative abundance was of 0.38 and 0.50 % for subsamples CA and CB. Other minor represented phylotypes found in the bacterial community structure of the CA and CB subsamples that have been reported for calcite precipitation were *Clostridium* and *Bacillus* (Gonzalez-Martinez et al. 2015a). *Clostridium* accounted for less than 0.01 % relative abundance in both subsamples, while *Bacillus* represented the 0.09 and 0.02 % in CA and CB subsamples, respectively. Therefore, microbial ecology analysis suggested that *Stenotrophomonas* genus was the major player in calcite precipitation in the CANON bioreactor.

The total relative abundance of reported phosphate-precipitating bacteria (0.40–0.80 %) and calcite-precipitating bacteria (0.39–0.52 %) was low in relation with the whole bacterial community structure, which summed up to a total of 0.79–1.32 % of total potential crystal-forming bacteria in the system. In spite of this, their relative abundance seemed to be high for a system in which neither phosphate nor calcite precipitation becomes a crucial result of treatment. Obviously, dominant bacterial phylotypes in the system were affiliated to ammonium-oxidizing *Nitrosomonas* (22–40 %) and to anaerobic ammonium-oxidizing *Planctomycete* clone (15.00–15.70 %). In this sense, even though bacterial genera previously described with mineral precipitation had low relative abundance with respect to other species, their relative abundance seemed sufficient for them to develop hydroxyapatite and calcite precipitation in the CANON bioreactor.

In conclusion, the bacterial ecology analysis of a CANON bioreactor showed the presence of ammonium-oxidizing *Nitrosomonas* and *Planctomycete* clones related to anammox bacteria and a diversity of putative heterotrophs. Among the bacterial species found, a number could trigger the formation of phosphate and calcite minerals in the CANON bioreactor. The possible hydroxyapatite-producing *Candidatus Accumulibacter* had a relative abundance of 0.36–0.38 % and was the highest potential phosphate-precipitating bacteria in the system. With respect to calcite, the major producer was thought to be *Stenotrophomonas* with a 0.38–0.50 % relative abundance. Although our study demonstrated evidences that explain the bioprecipitation of hydroxyapatite and calcite minerals inside the granular biomass of a CANON bioreactor, our data cannot conclude a direct relationship between species and mineral formed, but it does show that the formation of minerals in autotrophic granular systems (CANON bioreactor) was directly associated with microbial activity and also that in the granular microbial community can be found several phylotypes (some even not isolated in pure culture) described as potential mineral-precipitating bacteria. In this context, it must be considered that the biomineralization is a very

complex biological process involving both biotic (microbial activity, EPS production, or cellular structure) and abiotic (pH, nutrient concentration, or temperature) factors. Moreover, the autotrophic granules formed in a CANON bioreactor are also a very complex habitat with many different phylotypes and microenvironments (i.e., anoxic and aerobic zones) where many different metabolic activities such as partial nitritation and anammox process take place at the same time. Consequently, new research has to be conducted in order to unravel the unknowns around mineral precipitation in autotrophic nitrogen removal systems and the diversity of microorganisms that can produce it.

Acknowledgments The authors would like to acknowledge the support offered by the various institutions involved in this research, namely the Department of Built Environment of the Aalto University; the Institute of Water Research, the Department of Microbiology, and the Department of Mineralogy and Petrology of the University of Granada; and the Institute of Nanoelectronics of the University of Munich.

Compliance with ethical standards

Conflict of interest The authors declare that they have no conflict of interest.

Ethical approval This article does not contain any studies with human participants or animals performed by any of the authors.

References

Ali M, Okabe S (2015) Anammox-based technologies for nitrogen removal: advances in process start-up and remaining issues. Chemosphere 141:144–153

Aloisi G, Gloter A, Krüger M, Wallman K, Guyot F, Zuddas P (2006) Nucleation of calcium carbonate on bacterial nanoglobules. Geology 34:1017–1020

Barwell LJ, Isaac NJB, Kunin WE (2015) Measuring β-diversity with species abundance data. J Anim Ecol 84:1112–1122

Cha IT, Park SJ, Kim SJ, Kim JG, Jung MY, Shin KS, Kwon KK, Yang SH, Seo YS, Rhee SK (2016) *Marinoscillum luteum sp. nov.*, isolated from marine sediment. Int J Syst Evol Microbiol 63:3475–3480

Crutchik D, Garrido JM (2016) Kinetics of the reversible reaction of struvite crystallization. Chemosphere 154:567–572

Crystale J, Ramos DD, Dantas RF, Junior AM, Lacorte S, Sans C, Esplugas S (2016) Can activated sludge treatments and advanced oxidation processes remove organophosphorous flame retardants? Environ Res 144:11–18

Driscoll CT, Chen CY, Hammerschmidt CR, Mason RP, Gilmour CC, Sunderland EM, Greenfield BK, Buckman KL, Lamborg CH (2012) Nutrient supply and mercury dynamics in marine ecosystems: a conceptual model. Environ Res 119:118–131

Dupraz C, Visscher PT, Baumgartner LK, Reid RP (2004) Microbe-mineral interactions: early carbonate precipitation in a hypersaline lake (Eleuthera Island, Bahamas). Sedimentology 51:745–765

Edgar RC, Haas BJ, Clemente JC, Quince C, Knight R (2011) UCHIME improves sensitivity and speed of chimera detection. Bioinformatics 27:2194–2200

Elrich HL, Newman DK (2009) Geomicrobiology, 5th edn. CRC Press, New York

Gonzalez-Martinez A, Poyatos JM, Hontoria E, Gonzalez-Lopez J, Osorio F (2011) Treatment of effluents polluted by nitrogen with new biological technologies based on autotrophic nitrification-denitrification processes. Rec Pat Biotechnol 5:74–84

Gonzalez-Martinez A, Leyva-Díaz JC, Rodriguez-Sanchez A, Muñoz-Palazon B, Rivadeneyra A, Poyatos JM, Rivadeneyra MA, Martinez-Toledo MV (2015a) Isolation and characterization of bacteria associated with calcium carbonate and struvite precipitation in a pure moving bed biofilm reactor-membrane biorreactor. Biofouling 31:333–348

Gonzalez-Martinez A, Rodriguez-Sanchez A, Muñoz-Palazon B, Garcia-Ruiz MJ, Osorio F, van Loosdrecht MCM, Gonzalez-Lopez J (2015b) Microbial community analysis of a full-scale DEMON bioreactor. Bioprocess Biosyst Eng 38:499–508

Gonzalez-Martinez A, Rodriguez-Sanchez A, Garcia-Ruiz MJ, Muñoz-Palazon B, Cortes-Lorenzo C, Osorio F, Vahala R (2016a) Performance and bacterial community dynamics of a CANON bioreactor acclimated from high to low operational temperatures. Chem Eng J 287:557–567

Gonzalez-Martinez A, Rodriguez-Sanchez A, Lotti T, Garcia-Ruiz MJ, Osorio F, Gonzalez-Lopez J, van Loosdrecht MCM (2016b) Comparison of bacterial communities of conventional and A-stage activated sludge systems. Nature Sci Rep 6:18786

Haegeman B, Hamelin J, Moriarty J, Neal P, Dushoff J, Weitz JS (2013) Robust estimation of microbial diversity in theory and in practice. ISME J 7:1092–1101

Hao X, Heijnen JJ, Van Loosdrecht MCM (2002) Sensitivity analysis of a biofilm model describing a one-stage completely autotrophic nitrogen removal (CANON) process. Biotechnol Bioeng 77:266–277

Huse SM, Welch DM, Morrison HG, Sogin ML (2010) Ironing out the wrinkles in the rare biosphere through improved OTU clustering. Environ Microbiol 12:1889–1898

Huy H, Jin L, Lee Y-K, Lee KC, Lee J-S, Yoon J-H, Ahn CY, Oh HM (2013) *Arenimonas daechungensis sp. nov.*, isolated from the sediment of a eutrophic reservoir. Int J Syst Evol Microbiol 63:484–489

Kwon SW, Kim BY, Weon HY, Baek YK, Go SJ (2007) *Arenimonas donghaensis* gen. nov., sp. nov., isolated from seashore sand. Int J Syst Evol Microbiol 57:954–958

Lin YM, Lotti T, Sharma PK, Van Loosdrecht MCM (2013) Apatite accumulation enhances the mechanical property of anammox granules. Water Res 47:4556–4566

Lu Y-Z, Wang H-F, Kotsopoulos TA, Zeng RJ (2016) Advanced phosphorous recovery using novel SBR system with granular sludge in simultaneous nitrification, denitrification and phosphorous removal process. Appl Microbiol Biotechnol 100:4367–4374

Luo C, Wu D (2015) Environment and economic risk: an analysis of carbon emission market and portfolio management. Environ Res. doi:10.1016/j.envres.2016.02.007

Mañas A, Pocquet M, Biscans B, Sperandio M (2012) Parameters influencing calcium phosphate precipitation in granular sludge sequencing batch reactor. Chem Eng Sci 77:165–175

Martin JD (2004) Using XPowder—a software package for powder X-ray diffraction analysis. D.L. GR-1001/04.ISBN: 84–609–1497-6. Spain; 105 pp.

Omelon S, Ariganello M, Bonucci E, Grynpas M, Nanci A (2013) A review of phosphate mineral nucleation in biology and geobiology. Calcif Tissue Int 93:382–396

Oyserman BO, Noguera DR, Glavina Del Rio T, Tringe SG, McMahon KD (2015) Metatranscriptomic insights on gene expression and regulatory controls in *Candidatus Accumulibacter phosphatis*. ISME J: 1–13

Park H, Rosenthal A, Ramalingam K, Fillos J, Chandran K (2010) Linking community profiles, gene expression and N-removal in anammox bioreactors treating municipal anaerobic digestion reject water. Environ Sci Technol 44:6110–6116

Park JM, Park SJ, Ghim SY (2013) Characterization of three antifungal calcite-forming bacteria, Arthrobacter nicotianae KNUC2100, *Bacillus thuringiensis* KNUC2103, and *Stenotrophomonas maltophilia* KNUC2106, derived from the Korean Islands, Dokdo and their application on mortar. J Microbiol Biotechnol 23:1269–1278

Rivadeneyra MA, Martin-Algarra A, Sanchez-Roman M, Sanchez-Navas A, Martin-Ramos D (2010) Amorphous caphosphate precursors for Ca-carbonate biominerals mediated by *Chromohalobacter marismortui*. ISME J 4:922–932

Rivadeneyra A, Gonzalez-Martinez A, Gonzalez-Lopez J, Martin-Ramos D, Martinez-Toledo MV, Rivadeneyra MA (2014) Precipitation of phosphate minerals by microorganisms isolated from fixed-biofilm reactor used for the treatment of domestic wastewater. Int J Environ Res Public Health 11:3689–3704

Rodriguez-R LM, Konstantinidis KT (2014a) Estimating coverage in metagenomic data sets and why it matters. ISME J 8:1–3

Rodriguez-R LM, Konstantinidis KT (2014b) Nonpareil: a redundancy-based approach to assess the level of coverage in metagenomic datasets. Bioinformatics 30:629–635

Rusznyák A, Akob DM, Nietzsche S, Eusterhues K, Totsche KU, Neu TR, Frosch T, Popp J, Keiner R, Geletneky J, Katzschmann L, Schulze ED, Küsel K (2012) Calcite biomineralization by bacterial isolates from the recently discovered pristine karstic Herrenberg cave. Appl Environ Microbiol 78:1157–1167

Schloss PD, Westcott SL, Ryabin T, Hall JR, Hartmann M, Hollister EB, Lesniewski RA, Oakley BB, Parks DH, Robinson CJ, Sahl JW, Stres B, Thallinger GG, Van Horn DJ, Weber CF (2009) Introducing mothur: open-source, platform-independent, community-supported software for describing and comparing microbial communities. Appl Environ Microbiol 75:7537–7541

Seo HS, Kwon KK, Yang SH, Lee HS, Bae SS, Lee JH, Kim SJ (2009) *Marinoscillum gen. nov.*, a member of the family "*Flexibacteraceae*", with *Marinoscillum pacificum sp. nov.* from a marine sponge and *Marinoscillum furvescens nom. rev*, *comb. nov.* Int J Syst Evol Microbiol 59:1204–1208

Soares A, Veesam M, Simoes F, Wood E, Parsons SA, Stephenson T (2014) Bio-struvite: a new route to recover phosphorous from wastewater. Clean Soil Air Water 42:994–997

Tamura K, Stecher G, Peterson D, Filipski A, Kumar S (2013) MEGA6: molecular evolutionary genetics analysis version 6.0. Mol Biol Evol 30:2725–2729

Uad I, Gonzalez-Lopez J, Silva-Castro GA, Gonzalez-Martinez A, Martin-Ramos D, Rivadeneyra A, Rivadeneyra MA (2014) Precipitation of carbonate crystals by bacteria isolated from a sumerged fixed-film biorreactor used for the treatment of urban wastewater. Int J Environ Res 8:435–446

Wang C-C, Lee P-H, Kumar M, Huang Y-T, Sung S, Lin J-G (2010) Simultaneous partial nitrification, anaerobic ammonium oxidation and denitrification (SNAD) in a full-scale landfill-leachate treatment plant. J Hazard Mat 175:622–628

Winkler MKH, Kleerebezem R, Strous M, Chandran K, van Loosdrecht MCM (2013) Factors influencing the density of aerobic granular sludge. Appl Microbiol Biotechnol 97:7459–7468

Xing B-S, Guo Q, Jian X-Y, Chen Q-Q, Li P, Ni W-M, Jin R-C (2016) Influence of preservation temperature on the characteristics of an-aerobic ammonium oxidation (anammox) granular sludge. Appl Microbiol Biotechnol 100:4637–4649

Xu G, Zhou Y, Yang Q, Lee ZM-L, Gu J, Lay W, Cao Y, Liu Y (2015) The challenges of mainstream deammonification process for municipal used water treatment. App Microbiol Biotechnol 99:2485–2490

Yamagishi T, Takeuchi M, Wakiya Y, Waki M (2013) Distribution and characterization of anammox in a swine wastewater activated sludge facility. Water Sci Technol 67:2330–2336

Yoon MH, Im WT (2007) *Flavisolibacter ginsengiterrae gen. nov.*, *sp. nov.* and *Flavisolibacter ginsengisoli sp. nov.*, isolated from ginseng cultivating soil. Int J Syst Evol. Microbiol 57:1834–1839

Zhang X, Li D, Liang Y, Zhang Y, Fan D, Zhang J (2013) Application of membrane bioreactor for completely autotrophic nitrogen removal over nitrite (CANON) process. Chemosphere 93:2832–2838

Zhang L, Liu M, Zhang S, Yang Y, Peng Y (2015) Integrated fixed-biofilm activated sludge reactor as a powerful tool to enrich anammox biofilm and granular activated sludge. Chemosphere 140:114–118

Zhu G, Peng Y, Li B, Guo J, Yang Q, Wang S (2008) Biological removal of nitrogen from wastewater. Rev Environ Contam Toxicol 192: 159–195